Structure of Bacteriorhodopsin Investigated Using Fourier Transform Infrared Spectroscopy and Proteolytic Digestion†

David C. Lee, Eugenia Herzyk, and Dennis Chapman*

Department of Biochemistry and Chemistry, Royal Free Hospital School of Medicine, University of London, London NW3 2PF, U.K.

Received September 3, 1986; Revised Manuscript Received March 19, 1987

ABSTRACT: Fourier transform infrared spectra of purple membranes were examined by derivative and deconvolution methods to observe overlapping components of the amide I and II bands. Samples were studied in H_2O and ^2H_2O buffers and after drying. The spectra reveal a predominant α-helical conformation with some β-strand at least some of which adopts an antiparallel arrangement. Hydrogen–deuterium exchange of purple membranes results in a shift of an amide I component assigned to unordered structure and reveals the major amide I absorption frequency close to that calculated for an α_{II}-helical structure. The location of the β-structure was investigated by examination of the FTIR spectra of purple membranes after treatment with papain. These spectra showed that the β-strand remains after removal of the C-tail, the N-terminal region, and a loop between transmembrane segments 2 and 3. The data indicate that the absorption bands assigned to β-strand are not due to inaccurate subtraction of the absorption of background water or to the presence of residual tightly bound water in dried samples. This β-strand structure is closely associated with the lipid bilayer and is not exposed to proteolytic digestion.

Bacteriorhodopsin is the single protein of the purple membrane of *Halobacterium halobium* (Oesterhelt & Stoeckenius, 1971). Light energy is utilized by bacteriorhodopsin to translocate protons across the plasma membrane, setting up an electrochemical gradient that is utilized by the cell to synthesize ATP (Stoecknius et al., 1979). This protein, which is readily isolated, provides a model for understanding membrane-transport processes. As a first step in understanding function, many studies using microscopy, spectroscopy, and chemical treatments have been made to determine the structure of this transmembrane protein.

The generally accepted model for the structure of bacteriorhodopsin, derived principally from X-ray and electron diffraction measurements on purple membrane films, is of seven transmembrane α-helices slightly tilted with respect to the membrane normal (Blaurock, 1975; Henderson, 1975; Unwin & Henderson, 1975; Henderson & Unwin, 1975). A predominantly α-helical structure has been confirmed by circular dichroism (CD)[1] (Long et al., 1977; Muccio & Cassim, 1979) and infrared (IR) spectroscopies (Rothschild & Clark, 1979; Cortijo et al., 1982; Lee et al., 1985). However, Jap et al. (1983) by examination of an electron diffraction map at 3.7-Å resolution, the CD spectrum of purple membrane suspensions, and the IR spectrum of air-dried films proposed a model based on five α-helices and four strands of β-structure.

Infrared spectroscopy is an established technique for structural studies of biological systems (Susi, 1969; Alix et al., 1985). The routine use of microcomputers for the subtraction of background water absorptions (Chapman et al., 1980) has permitted the study of soluble proteins (Koenig & Tabb, 1980) and membrane systems (Lee & Chapman, 1986). The most commonly used absorptions for the analysis of protein structure are the amide I and II bands arising from delocalized vibrations of the peptide grouping (Susi, 1969). Both theoretical and experimental studies have shown that α-helical, β-strand, and random conformations in polypeptides and proteins may be distinguished by the frequency of the amide I absorption maximum (Krimm, 1962; Susi et al., 1967; Timasheff et al., 1967; Susi, 1969; Koenig & Tabb, 1980). However, the bandwidths of the amide I absorptions of these different structures are greater than the separation between them. In order to observe these overlapping bands in the IR spectra of proteins and membranes, derivative (Susi & Byler, 1983; Lee et al., 1985), deconvolution (Yang et al., 1985; Olinger et al., 1986), and curve-fitting (Ruegg et al., 1975; Jap et al., 1983) approaches have been used.

Enzymatic cleavage of bacteriorhodopsin in purple membranes has been used by several authors to determine the amino acid sequence and the topography of the protein in the membrane (Ovchinnikov et al., 1979, 1984; Gerber et al., 1977, 1979; Khorana et al., 1979; Walker et al., 1979; Huang et al., 1981; Katre & Stround, 1981) and the structure and flexibility of the exposed C-tail (Wallace & Henderson, 1982; Wallace & Kohl, 1984; Renthal et al., 1983) as well as the localization of the retinal (Katre et al., 1981; Ovchinnikov et al., 1984) and antigenic binding sites (Kimura et al., 1982). The role of the C-tail of bacteriorhodopsin in proton-pumping activity has also been investigated by enzymatic digestion (Abdulaev et al., 1978; Huang et al., 1981; Govindjee et al., 1982; Liao & Khorana, 1984; Ovchinnikov et al., 1986). Taking into consideration the number of cleavage sites and the amount of material removed from the membrane, papain is the most effective enzyme in comparison with trypsin, carboxypeptidase A, pronase, lactoperoxidase, chymotrypsin, or thermolysin (Gerber et al., 1977; Abdulaev et al., 1978; Ovchinnikov et al., 1984; Liao & Khorana, 1984).

† This work was supported by the Wellcome Trust.

[1] Abbreviations: A_{II}/A_I, amide II/amide I band intensity ratio; CD, circular dichroism; IR, infrared; FTIR, Fourier transform infrared; EDTA, ethylenediaminetetraacetic acid; PMSF, phenylmethanesulfonyl fluoride; HEPES, *N*-(2-hydroxyethyl)piperazine-*N*′-2-ethanesulfonic acid; HPLC, high-pressure liquid chromatography; M_r, relative molecular mass; TFA, trifluoroacetic acid; SDS–PAGE, sodium dodecyl sulfate–polyacrylamide gel electrophoresis.

0006-2960/87/0426-5775$01.50/0

In this paper we present an FTIR study of purple membranes in H_2O and ^2H_2O and dried in the presence and absence of glucose. These spectra are analyzed by second and fourth derivatives and deconvolution. By this means we establish whether the band observed at 1630–1640 cm^{-1} is a genuine protein absorption or is due to poor water subtraction or residual bound water in dried samples. We have also recorded FTIR spectra of bacteriorhodopsin after incubation with papain in an attempt to correlate changes in the spectra with the removal of known structural features. Such an approach may provide a means of localizing the structural features giving rise to the 1630–1640-cm^{-1} amide I absorption, which has been assigned to the presence of β-structure (Cortijo et al., 1982; Jap et al., 1983; Lee et al., 1985).

Materials and Methods

Preparation of Purple Membrane. H. halobium (R_1 strain) was obtained from the American Type Culture Collection (Rockville, MD) and grown on a complex medium of salt and bacteriological peptone according to the method of Oesterhelt and Hartman (1979). Purple membrane was purified according to Oesterhelt and Stoeckenius (1974) using two gradient centrifugation steps to ensure complete separation of red membranes from purple membranes. Gradients were continuous 25–60% sucrose. The final purple fractions were pooled, washed three times by centrifugation (100000*g* for 30 min) in distilled water, and stored frozen. All spectra were recorded with light-adapted purple membranes.

Papain Digestion of Bacteriorhodopsin in Purple Membranes. Purple membranes (0.5 mg of protein/mL) were digested with papain (Sigma type IV, 23 units/mg of protein) in a buffer similar to that used by Katre et al. (1981), containing 1.0 mM EDTA, 0.08 mM 2-mercaptoethanol, and 5.5 mM cysteine hydrochloride, pH 6.8. The suspension was incubated at 37 °C and a solution of papain added to a final ratio of 1:200 papain to bacteriorhodopsin by weight. The mixture was sampled for analysis after 2 h of incubation after which the papain concentration in the digest was increased to a final weight ratio of 1:2. A final sample was taken after 24 h of incubation. Digestion was stopped after 2 and 24 h by addition of 20 mM phenylmethanesulfonyl fluoride (PMSF) to a final concentration of 10 μm followed by immediate centrifugation (130000*g*, 15 min). The supernatants were collected for HPLC measurements and the pellets washed once in 1 M KCl and 10 mM HEPES, pH 6.8, by centrifugation and resuspended in this buffer to a concentration of 6–12 mg of protein/mL. Washing the pellets with buffer rather than water was found to be necessary for removing papain from samples digested for 24 h at 1:2.

SDS–Polyacrylamide Gel Electrophoresis. The untreated and papain-digested bacteriorhodopsin in purple membranes were subjected to electrophoresis on a polyacrylamide gel (3% stacking gel, 18% separating gel) containing 0.1% sodium dodecyl sulfate according to the method of Laemmli (1970). The fixing and staining procedure for the gel was as follows: 12 h in 10% acetic acid and 25% isopropyl alcohol; 12 h in 10% acetic acid, 25% isopropyl alcohol, and 0.025% Coomassie blue; 12 h in 10% acetic acid, 10% isopropyl alcohol, and 0.0025% Coomassie blue followed by several washes of a few hours in a 10% acetic acid destaining solution. Carbonic anhydrase (29 000), trypsin inhibitor (20 100), and α-lactalbumin (14 200) were used as molecular weight markers.

Visible and Fluorescence Spectra. The visible absorption and fluorescence emission spectra of untreated and papain-digested purple membranes (1 mg of bacteriorhodopsin/mL in water suspension) were recorded at 20 °C with a Pye Unicam SP8-100 spectrophotometer and a Perkin-Elmer LS-5 luminescence spectrometer with 3600 Data Station (excitation wavelength 280 nm), respectively. The pH of the samples was checked and adjusted if necessary to pH 6.8 by small aliquots of HCl or NaOH prior to measurement.

HPLC Measurements. The supernatants obtained after centrifugation of papain-digested purple membranes (1.3 mg of bacteriorhodopsin) were lyophilized, and low molecular weight peptides were extracted by the following procedure: (a) addition of 500 μL of 0.1% TFA to the powder; (b) centrifugation at 10000*g* for 5 min; (c) lyophilization of the supernatant; (d) dissolution of the powder in 100 μL of 0.1% TFA.

The pellets obtained from the centrifugation of digested purple membranes were washed once in 1 M KCl and 10 mM HEPES, pH 6.8, and lyophilized. The powder was resuspended in 1 mL of H_2O, and several lipid extractions were performed using 1-mL aliquots of chloroform. The aqueous fractions were lyophilized and treated according to the procedures a–d.

The final extracts in 0.1% TFA were fractionated by reversed-phase HPLC (Altex system with a Model 420 solvent programmer) using a C18 column (300-Å pore size, 4.6 × 250 mm, Aquapore RP-300, Brownlee). The separation was performed with a flow rate of 1 mL/min with an acetonitrile gradient of 5–90%. Absorbance was monitored at 220 nm.

Fourier Transform Infrared Spectroscopy. For infrared spectroscopy all samples in H_2O were washed and resuspended in 1 M KCl and 10 mM HEPES, pH 6.8. Hydrogen–deuterium exchange of purple membranes was accomplished by washing of purple membranes in 10 mM HEPES and 1 M KCl, p^2H 6.8, by centrifugation (3× 1:10 dilution of H_2O present in original sample) followed by incubation at room temperature and elevated temperatures. The spectra of aqueous samples were recorded at a concentration of 6–13 mg of bacteriorhodopsin/mL. Drying of purple membranes was carried out by freeze drying at −60 °C (6.3 mmHg) from suspensions in water or 0.5% glucose. Dry samples were recorded as KBr disks. Lyophilized powder (2–4 mg) was mixed thoroughly with ca. 100 mg of dried and ground KBr followed by pressing at 10 tons for 20 min under vacuum.

Infrared spectra were recorded on a Perkin-Elmer 1750 FTIR spectrometer equipped with a fast-recovery TGS detector and Perkin-Elmer 7300 computer for data aquisition and analysis. Aqueous samples were placed in a thermostated Beckman FH-01 CFT microcell fitted with CaF_2 windows and a 6-μm tin spacer. The temperature of the sample was controlled by means of a cell jacket of circulating water. Temperature calibration via a thermocouple placed against a cell window was better than 0.5 °C. The spectrometer was continuously purged with dry air to eliminate water vapor absorptions from the spectral region of interest. A sample shuttle was used to allow the background spectrum to be averaged over the period of data collection. For the aqueous samples 400 scans were coadded, apodized with a medium Norton–Beer function, and Fourier transformed to give a resolution of 4 cm^{-1}. For samples prepared as KBr disks 64 scans were coadded.

Buffer spectra were recorded in the same cell and under the same instrument conditions as sample spectra. Difference spectra were generated by an interactive difference (IDIFF) routine to subtract the spectrum of the aqueous buffer from the spectrum of the membrane suspension. The same procedure was applied in the case of the samples recorded as KBr disks using the spectrum recorded from a blank KBr disk to

allow for any residual water. Proper subtraction of water was judged to yield an approximately flat base line at 1900–1480 cm^{-1}, avoiding negative sidelobes. Subtraction of ^2H_2O was adjusted to the removal of the ^2H–O–^2H bending absorption near 1220 cm^{-1}. Second- and fourth-derivative spectra were generated from difference spectra by an OBEY program supplied by Perkin-Elmer. In order to reduce noise, the rate of change of slope (second derivative) was calculated over a 13-data-point (13-cm^{-1}) range and this repeated to yield the fourth derivative. Spectral deconvolution was performed by Perkin-Elmer's ENHANCE function, which is analogous to the method of Kauppinen et al. (1981). Deconvolution parameters used for the amide I band were σ = 7.5 cm^{-1} (half-width at half-height) and K = 2.25 (relative reduction in bandwidth).

RESULTS

Infrared Spectrum of Purple Membranes in Suspension. FTIR spectra of purple membranes suspended in H_2O and ^2H_2O buffer systems are presented in Figure 1. In H_2O the difference spectrum (see Figure 4a) reveals three major absorptions in the spectral region shown: the amide I band at 1661 cm^{-1}, the amide II band at 1546 cm^{-1}, and a C–H deformation absorption with a maximum at 1457 cm^{-1}. The amide I and II absorption bands cannot be assigned to single atomic displacements, although the amide I absorption is principally C=O stretching and the amide II principally N—H bending (Susi, 1969). The amide I frequency of 1661 cm^{-1} agrees closely with previous reports and has been assigned to distorted (Rothschild & Clark, 1979) or α_{II}-helices (Krimm & Dwivedi, 1982). The amide II band frequency of 1546 cm^{-1} is also indicative of a major structural contribution from α-helices (Susi et al., 1967). Careful examination of the absorption spectrum reveals amide I shoulders near 1690, 1630–1640, and 1620 cm^{-1} and an amide II shoulder near 1515 cm^{-1}. Three methods of data analysis were used with the aim of determining the number and position of any overlapping amide components. Absorption bands in the original difference spectrum are revealed as negative bands in the second-derivative spectrum presented in Figure 1a (lower). Amide I components are present at 1685, 1661, 1636, and 1619 cm^{-1}. The amide II band splits into two components at 1548 and 1517 cm^{-1}. In the fourth-derivative spectrum (not shown) amide I bands are revealed at 1685, 1661, 1636, and 1619 cm^{-1} with amide II bands at 1549, 1530, and 1517 cm^{-1}. An independent method for analyzing overlapping band shapes is provided by spectral deconvolution (Kauppinen et al., 1981), which presents amide I components at 1684, 1675 (sh), 1661, 1637, and 1619 cm^{-1} and amide II components at 1548 and 1517 cm^{-1} (Figure 1a, upper). Each of these methods of data analysis results in a reduced signal-to-noise ratio. The spectral region 1900–1800 cm^{-1}, which is free from sample absorption, is presented for comparison with the amide I and II regions. In this work, amide components of comparable intensity to the "bands" in the 1900–1800-cm^{-1} region will not be considered for assignment.

Aside from the predominant α-helical conformation that may be deduced from the difference spectrum, the component at 1636 cm^{-1} may be assigned to the presence of some β-strand structure in this protein (Susi et al., 1967; Susi & Byler, 1983). The presence of a component at 1685 cm^{-1} indicates either that neighboring β-strands are antiparallel in orientation (Krimm, 1962; Susi et al., 1967) or that β-turns are present (Bandekar & Krimm, 1980). The band at 1619 cm^{-1} (1617 cm^{-1} in ^2H_2O) is outside the frequency range normally associated with protein secondary structure and could arise from an amino acid side-chain mode. A strong absorption has been

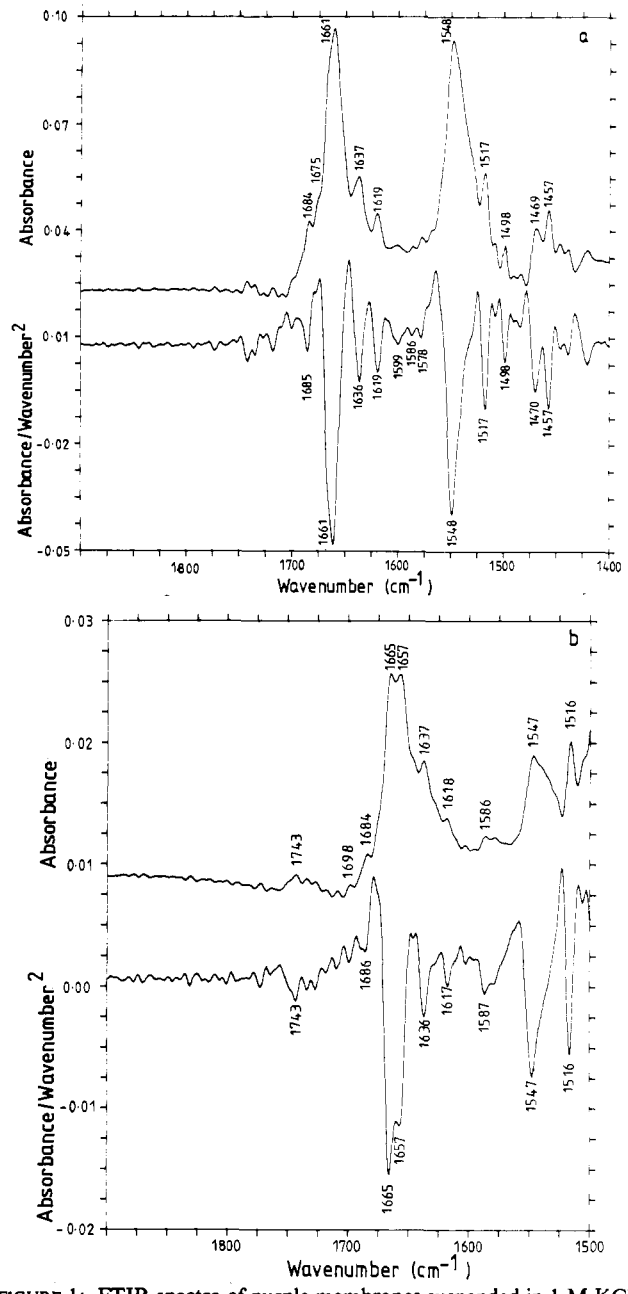

FIGURE 1: FTIR spectra of purple membranes suspended in 1 M KCl and 10 mM HEPES, pH 6.8 (a), or 1 M KCl and 10 mM HEPES, p^{2}H 6.8 (^2H_2O) (b), recorded at 20 °C. Deconvolved spectra (upper traces) and second-derivative spectra (lower traces) are shown. The sample in ^2H_2O buffer was incubated at 50 °C for 27 h to increase hydrogen–deuterium exchange before scanning.

detected in the range 1618–1615 cm^{-1} in solvent-denatured water-soluble proteins and was assigned to distorted β-strands (Purcell & Susi, 1984). The 1619–1617-cm^{-1} absorption was present in the FTIR spectra of all batches of purple membrane recorded under a variety of conditions, and it seems likely that it represents a further, native region of β-structure. The absorption at 1517 cm^{-1} has been assigned to tyrosine side chains (Chirgadze et al., 1975) though there may be some contribution from peptide groups in α-helical conformation or unordered segments (Krimm, 1962). The bands at 1470 and 1457 cm^{-1} may be assigned as C–H deformation modes arising from the lipid acyl chains (Asher & Levin, 1977) and amino acid side chains present.

FTIR spectra of purple membranes in ^2H_2O buffer are presented in Figure 1b. The extent of exchange as measured by the decrease in amide II/amide I ratio in the difference

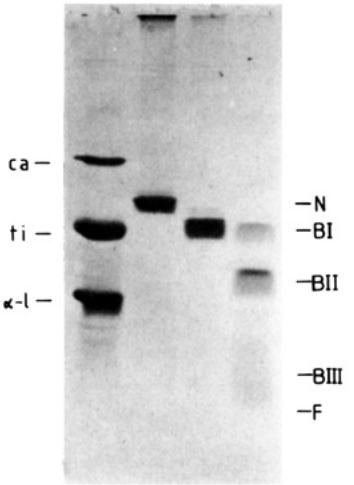

FIGURE 2: SDS–polyacrylamide gel of purple membranes after digestion with papain together with a control. The positions of the bands on the gel of native bacteriorhodopsin (N) and bacteriorhodopsin after papain digestion are shown: 2 h at 1:200 papain to bR (mg/mg) (BI); 24 h at 1:2 (mg/mg) (BI–BIII). A calibration plot was made according to molecular weight standards: carbonic anhydrase, 29 000 (ca); trypsin inhibitor, 20 100 (ti); α-lactalbumin, 14 200 (α-l). The front of the running gel is indicated by F. Details of sample preparation and staining procedure are in the text.

spectrum (A_{II}/A_I) was 79%. Incubation for longer periods to give greater exchange (up to 90%) gave no further band shifts. A control sample in H_2O incubated at 50 °C (not shown) revealed no band shifts compared to the spectra in Figure 1a.

The difference spectrum shows the amide I′ band at 1659 cm^{-1} with a shoulder near 1637 cm^{-1}, the residual amide II band at 1541 cm^{-1}, and a broad band centered at 1456 cm^{-1} representing overlap between amide II′ and C–H deformation modes (Susi, 1969). The second derivative (Figure 1b, lower) reveals amide I′ components at 1686, 1665, 1657, 1636, and 1617 cm^{-1} and amide II components at 1547 and 1516 cm^{-1}. The presence of these absorptions is confirmed by the deconvolved spectrum (Figure 1b, upper). The band at 1743 cm^{-1} may be due to the presence of a small proportion of lipid ester C=O groups (Asher & Levin, 1977).

Papain Cleavage of Bacteriorhodopsin. The typical pattern of SDS–PAGE of native and papain-treated bacteriorhodopsin is shown in Figure 2. After 2-h digestion at a 1:200 (mg/mg) ratio, bacteriorhodopsin gave a single band (BI). The shift of this band to lower molecular weight in comparison to native bacteriorhodopsin (N) indicates the removal of a peptide fragment of M_r 2000 from the protein. This corresponds closely to the molecular weight (M_r 1800) of the 17 amino acid C-tail (Ovchinnikov et al., 1984). The complete disappearance of a band corresponding to native bacteriorhodopsin indicates that all the protein molecules have been cleaved.

After 24-h digestion at a 1:2 (mg/mg) ratio, three bands are observed by SDS–PAGE—BI, BII, and BIII. The position of these bands indicates that the fragment BI produced after 2-h digestion has split into two fragments, BII (M_r ~16 000) and BIII, which ran at the dye front. Since 18% gel electrophoresis cannot separate proteins of M_r <12 000, the size of the fragment BIII was deduced by difference to have a M_r ~8000 (after removal of the C-tail bacteriorhodopsin has M_r ~24 000). An 8 M urea–SDS–12.5% polyacrylamide gel system was used to resolve oligopeptides of M_r 2500–17 000, revealing fragment BIII as a single band.

HPLC Measurements. HPLC analysis of the original supernatants and pellets obtained after washing of papain-digested purple membranes was performed to ensure that the samples used for FTIR analysis were free of small molecular weight fragments. The chromatograms are presented in Figure 3. The results show the presence of peptides in the supernatants but not in the pellets obtained after one wash. This indicates that the material cleaved from bacteriorhodopsin by digestion passed into solution on washing and was not present in the pellets that were resuspended for FTIR measurements.

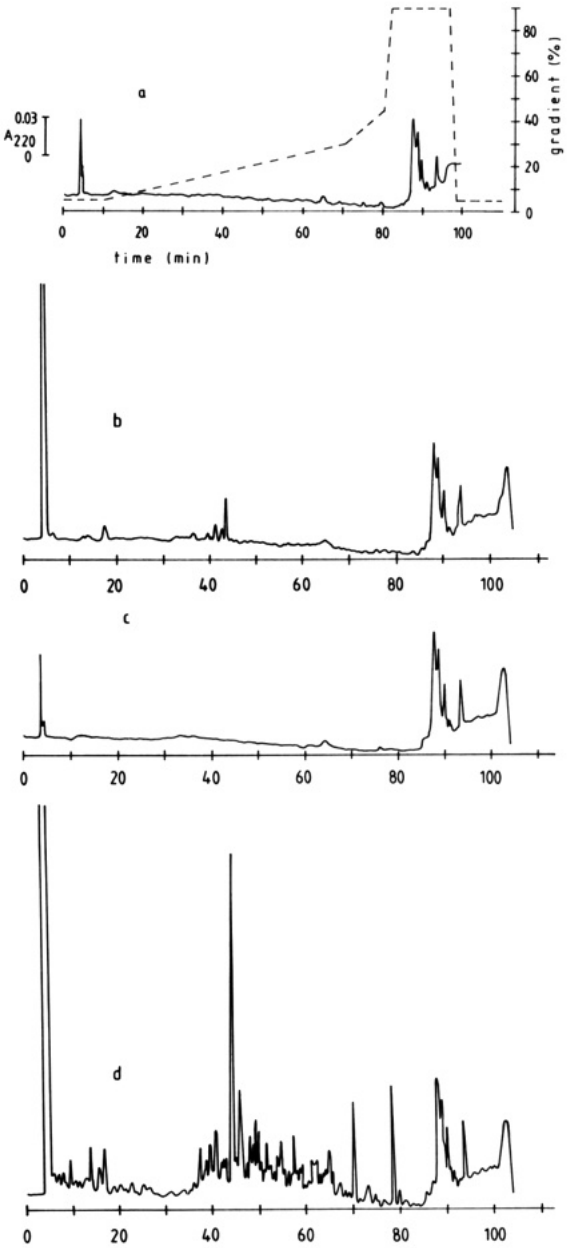

FIGURE 3: HPLC separation of peptides in once washed pellets (a, c) and first supernatants (b, d) obtained after centrifugation of papain-digested purple membrane samples: (a, b) 2-h digestion, 1:200 papain to bacteriorhodopsin (w/w); (c, d) 24-h digestion, 1:2. The absorbance scale and acetonitrile gradient are shown in (a).

Visible Absorption and Fluorescence Emission Spectra. The absorption maximum of bacteriorhodopsin remains unchanged at 562 nm after 2-h digestion (1:200 mg/mg) but shifts to 548 nm after 24-h digestion (1:2 mg/mg) with papain. The fluorescence emission spectra (upon excitation at 280 nm) gave a similar response. After 2-h digestion no change from 326 nm was observed, but a shift in emission maximum to 330 nm was observed after 24 h.

Shifts of the visible absorption maximum that occur, for example, during the photocycle (Lozier et al., 1975; Tokunaga

& Iwasa, 1982) or in response to changes in pH (Mowerey et al., 1979) are due to reorganization of the retinal chromophore attached to the protein (Nakanishi et al., 1980). It has been suggested that this reorganization may, in some cases, be due to conformational changes in the protein (Honig et al., 1976). This is supported by experimental data demonstrating the dependence of the absorption spectrum of a protonated Schiff base on the polarizibility and polarity of the solvent (Irving et al., 1970). Theoretical calculations have shown that the arrangement of polar and charged residues of the protein around the chromophore influences its spectral properties (Suzuki et al., 1974).

According to these considerations the shift of the absorbance maximum of bacteriorhodopsin after 24-h papain digestion suggests protein conformational changes in the region of the chromophore. However, cleavage of the C-tail after 2-h digestion does not produce any such conformational change according to the absence of changes in the visible spectrum.

This conclusion is supported by analysis of the fluorescence spectra of digested samples. The fluorescence emission spectra of proteins arise mainly from tryptophan and tyrosine residues and are dependent on the environment of these residues (Cowgill, 1963), which, in turn, is a reflection of conformation (Konev, 1967). A red shift of the emission spectrum, such as that observed after 24-h digestion with papain, is usually connected with an increase in polarity in the locality of tryptophan residues. No shift was observed after 2-h digestion. Thus, we may conclude that cleavage of the C-tail causes no conformational change in bacteriorhodopsin.

FTIR Spectra of Papain-Digested Purple Membranes. Figure 4a presents spectra of purple membranes after 2-h (1:200) and 24-h (1:2) digestion with papain and resuspension in 1 M KCl and 10 mM HEPES, pH 6.8. The subtraction factor used for the removal of background water absorption was chosen carefully to give approximately equivalent base lines for these spectra and for a spectrum of a control sample that is also shown. This allows changes in the relative intensity of band shoulders to be monitored with certainty. The principal effect of papain digestion was a progressive narrowing of the amide I band caused by a reduction in the intensity of the 1630–1640-cm^{-1} shoulder. The full amide I width at half-height (measured from a sloping linear base line 1728–1590 cm^{-1}) was 39 cm^{-1} (control), 33 cm^{-1} (2 h), and 26 cm^{-1} (24 h). Also observed was an increase in the relative intensity of the amide II band on papain digestion. The A_{II}/A_{I} ratios were 0.74 (control), 0.82 (2 h), and 0.85 (24 h). There was a shift in the position of the amide I band maximum from 1661 to 1662 cm^{-1} in the digested samples.

The second-derivative spectra of the papain-digested samples presented in Figure 4b reveal a major amide I component at 1663–1664 cm^{-1} and minor components at 1684–1690, 1635–1636, and 1619–1620 cm^{-1}. In the second derivative of the control spectrum the major amide I band was at 1661 cm^{-1}, but all other bands overlapped with those in the spectra of the digested samples. The deconvolved FTIR spectra are shown in Figure 4c. The decrease in the relative intensity of the 1630–1640-cm^{-1} band on digestion is clearly shown in these spectra. There was also a decrease in intensity at 1682 cm^{-1}. Again an increase in the band maximum frequency of the major amide I component from 1661 to 1663–1664 cm^{-1} was observed.

Second-derivative FTIR spectra of papain-digested purple membranes that were dried in the absence of glucose are presented in Figure 5. The major amide I band was found at 1659 cm^{-1} with weaker components at 1685, 1636, and

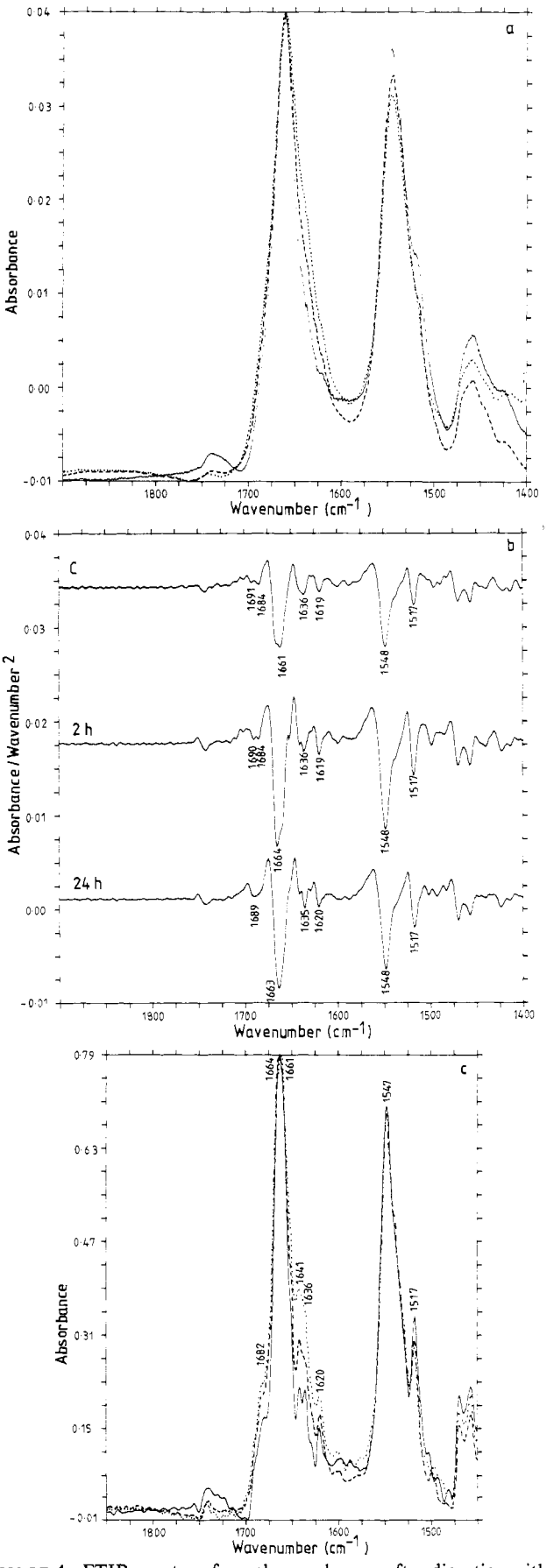

FIGURE 4: FTIR spectra of purple membranes after digestion with papain. Samples were washed once and resuspended in 1 M KCl and 10 mM HEPES, pH 6.8, and spectra recorded at 20 °C. (a) Difference spectra; (b) second-derivative spectra; (c) deconvolved spectra. For (a) and (c): control (dotted line); 2 h-digestion at 1:200 papain the bacteriorhodopsin (w/w) (broken line); 24-h digestion at 1:2 (solid line).

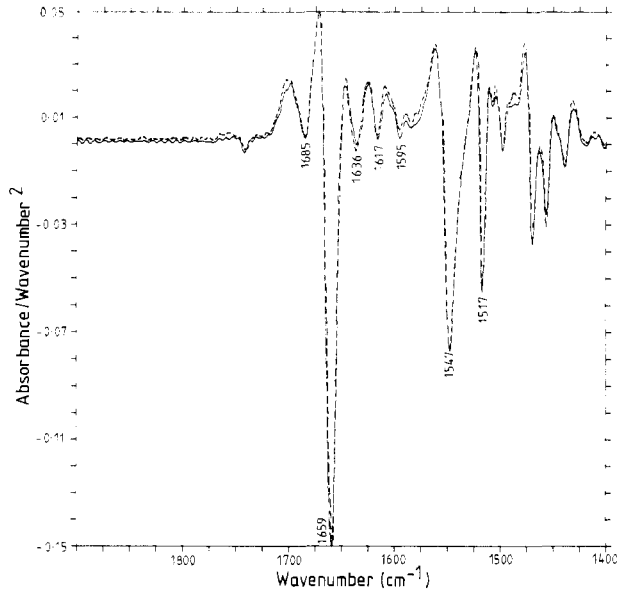

FIGURE 5: Second-derivative FTIR spectra of purple membranes after digestion with papain and lyophilization: 2-h digestion (broken line); 24-h digestion (solid line). Spectra were recorded from samples prepared as KBr disks.

1616–1617 cm^{-1}. Major amide II bands were at 1547 and 1517 cm^{-1}. The shift of the main amide I band from 1661 to 1659 cm^{-1} on drying could be prevented by the inclusion of 0.5% glucose in the medium before drying (data not shown). No shift of the components assigned to β-structure was observed under these conditions. Papain-digested membranes were also subjected to extensive hydrogen–deuterium exchange by incubation at 50 °C in ^2H_2O buffer as for the sample in Figure 1b. FTIR spectra of these samples digested for 2 or 24 h revealed absorptions at 1685 and 1635 cm^{-1} in addition to the main band at 1664 cm^{-1} (data not shown). Under these conditions, the bands that we assign to antiparallel β-strands were of equivalent intensity relative to the main α-helical absorption as for the spectra shown in Figures 4 and 5.

DISCUSSION

Structure of Bacteriorhodopsin in the Purple Membrane. Our study, by measurement of the main amide I and II peak frequencies after derivation and deconvolution of the FTIR spectrum, confirms that bacteriorhodopsin is principally an α-helical protein. Studies of α_I-poly(L-alanine) and α_{II}-poly(L-alanine) have shown that the amide I frequency of the α_{II}-helical structure is higher than that of the α_I-helix (Dwivedi & Krimm, 1984). The observed amide I frequency for bacteriorhodopsin is close to that calculated for the α_{II}-helix (Krimm & Dwivedi, 1982). Our studies of hydrogen–deuterium exchange provide further evidence for the presence of α_{II}-helical structure in this protein. Replacement of peptide group NH by N^{2}H results in a decrease in amide I frequency, the magnitude of which is dependent on the secondary-structure arrangement (Susi, 1969). Thus, the shift of the main amide I component from 1661 to 1665 cm^{-1} after extensive exchange must be due to the shift to lower frequencies of a minor component that now appears at 1657 cm^{-1}. In the spectra recorded from H_2O samples this band cannot be distinguished from the main band by either derivative or deconvolution calculations, and this overlap would cause the latter to appear at lower frequencies. The 1657-cm^{-1} band that appears during the initial stages of exchange is probably due to random structure or β-turn structure located on the outside of the membrane and therefore readily exchanged (Susi et al., 1967; Bandekar & Krimm, 1980; Olinger et al., 1986). The main band position in ^2H_2O of 1665 cm^{-1} is very close to the 1667-cm^{-1} value for α_{II}-helices calculated by Dwivedi and Krimm (1984).

The α_I- and α_{II}-helical structures have the same number of residues and the same rise per turn but differ in the dihedral angles ϕ and ψ (Dwivedi & Krimm, 1984). This means that in the α_{II}-helix the plane of the peptide group is tilted with respect to the helical axis such that the N–H bond points toward the axis. There is X-ray evidence for the presence of α-helical structures that have the dihedral angles of the α_{II}-structure in lysozyme (Blake et al., 1967) and α-chymotrypsin (Birktoft & Blow, 1972).

All the FTIR spectra of native purple membranes presented in this work display a low-frequency shoulder on the main amide I band. This absorption was detected in H_2O samples, ^2H_2O samples, and dried samples. The use of derivative and deconvolution methods enabled us to determine the position of this band as 1636 cm^{-1}. By comparison with spectra of polypeptides and soluble proteins of known structure (Susi et al., 1967; Koenig & Tabb, 1980; Susi & Byler, 1983) as well as theoretical calculations (Krimm, 1962; Krimm & Abe, 1972; Chirgadze & Nevskaya, 1976) we may confidently assign this absorption to the presence of β-strand in bacteriorhodopsin.

Although this absorption has been detected in several other IR analyses of the structure of bacteriorhodopsin (Rothschild & Clark, 1979; Cortijo et al., 1982; Jap et al., 1983; Lee et al., 1985; Nabedryk et al., 1985; Downer et al., 1986), because the accepted structural model does not include β-strand several explanations have been proposed. Poor subtraction of background water absorption in aqueous samples and the presence of residual tightly bound water in dried samples (Nabedryk et al., 1985) have been suggested as the origin of the low-frequency amide I shoulder. These possibilities are eliminated by this study as the absorption is present in our spectra recorded after 79% H–^{2}H exchange when all H_2O has been removed from the sample.

An alternative explanation for these absorptions comes from a recent study of several soluble proteins of known structure using deconvolved FTIR spectra (Byler & Susi, 1986). The spectra of the highly helical proteins hemoglobin and myoglobin revealed minor absorptions around 1627–1638 and 1671–1675 cm^{-1} in ^2H_2O. As neither of these proteins contain β-structure, these absorptions must be associated with the chains interconnecting the helices and were described by these workers as possibly due to strong interactions between neighboring C=O oscillators. It is possible that similar interconnecting segments between helices could give rise to the absorptions in this region observed in the spectra of bacteriorhodopsin. However, we discount this possibility as a comparison with the spectrum of hemoglobin (our unpublished data) indicates that the related absorptions of bacteriorhodopsin are much stronger. Additionally the positions of the bands are not shifted after 79% hydrogen–deuterium exchange as would be expected for extended segments (Susi et al., 1967; Susi, 1969).

A further clue to the presence of β-structure comes from the presence of the higher frequency component of the amide I absorption of β-strands (Susi, 1969). This is expected near 1690 cm^{-1} for antiparallel strands or near 1648 cm^{-1} for parallel strands (Krimm, 1962; Susi et al., 1967). Parallel-chain conformation may not be detected in this study because of overlap with strong α-helical absorptions. The presence of the 1685-cm^{-1} absorption (Figure 1) suggests that at least some

of the β-strand forms antiparallel chains. However, assignment of absorptions in this region is complicated by the possibility of contribution from β-turn modes (Bandekar & Krimm, 1979, 1980). A distinction between these absorptions may be made by examining the spectrum under conditions of partial deuteriation (Olinger et al., 1986). Turn structures are expected to be located on the exterior of the membrane and therefore readily deuteriated. Partial deuteriation (59%, not shown) of bacteriorhodopsin resulted in no shift of the high-frequency amide I component at 1685 cm^{-1}. Studies of ribonuclease have shown the absorption of deuteriated turn structures to be below 1680 cm^{-1} (Olinger et al., 1986; Haris et al., 1986), and we therefore assign the 1685-cm^{-1} absorption after partial deuteriation to antiparallel β-strands. In H_2O this absorption may be due to β-turn structures as well as antiparallel β-strands.

A recent polarized IR study of purple membrane films (Nabedryk et al., 1985) was interpreted to suggest that any β-strand, if present, was not oriented perpendicular to the membrane. The expected negative dichroism for the amide I absorption of such β-structure was not detected although this may have been due to band overlap with the positive absorption of α-helices. A structural analysis using solid-state nuclear magnetic resonance has shown that the experimentally observed line shape is consistent either with a structure entirely comprised of α_I-helices tilted 20° from the membrane normal or with a 60% α_{II}-helical (perpendicular to the normal) and 40% antiparallel β-sheet (tilted 10–20° from the normal) structure (Lewis et al., 1985). Our studies of the FTIR spectra of native purple membranes under a variety of conditions and using different methods of band analysis have shown that bacteriorhodopsin contains a proportion of β-structure in addition to the predominant α-helical structure. In order to assist the location of this β-structure in the protein, we used a combination of proteolytic digestion using papain and FTIR.

Papain Digestion of Bacteriorhodopsin in Purple Membranes. The 17 amino acid C-tail of bacteriorhodopsin is completely removed by papain after 2-h incubation at 37 °C and an enzyme to protein (w/w) ratio of 1:200 (Ovchinnikov et al., 1979, 1984; Abdulaev et al., 1978; Renthal et al., 1983). According to Ovchinnikov's data the use of higher concentrations of papain (1:20 to 1:1) and longer incubation times (up to 24 h) leads to the removal of three amino acids from the N-terminus and a fragment between amino acids 66–72 connecting the second and third transmembrane segment of bacteriorhodopsin. The accessibility of these regions to papain treatment indicates that they are exposed to the external medium. It has been suggested that amino acids 66–72 form a loop that protrudes from the membrane (Ovchinnikov et al., 1979). The peptides cleaved by papain form 11% of the 248 amino acids of the protein. Further incubation (up to 7 days) did not result in further digestion of the protein. However this does not provide proof that all other segments are embedded in the membrane. Indeed an antigenic determining site distinct from the C-tail has been found and is thought to be exposed between transmembrane segments 3 and 4 (Kimura et al., 1982).

The formation of fragments of M_r 16 000 and 8000 after prolonged exposure to papain (Figure 2) agrees with the data of Ovchinnikov et al. (1984). However, we did not obtain cleavage of the entire sample as band BI was still present after prolonged digestion (up to 7 days at 1:20 papain to bacteriorhodopsin) or the use of higher papain concentration (1:1) (data not shown).

The estimation of the molecular weight of bacteriorhodopsin fragments formed by papain digestion using SDS–PAGE should be regarded as approximate since native bacteriorhodopsin gave a molecular weight of 22 500 ± 500 (six experiments) whereas a value of 26 000 has been obtained from the amino acid composition (Ovchinnikov et al., 1979; Khorana et al., 1979). This problem has been noted by several authors [for example, Bridgen and Walker (1976), Abdulaev et al. (1978), and Wallace and Henderson (1982)].

HPLC analysis was used to confirm the removal of small molecular weight peptides from the samples used for FTIR measurements after papain digestion. Thus structural features deduced from the spectra can be unequivocally assigned to the segments remaining in the membrane. Additionally, the number of peaks obtained from the supernatant after 2-h digestion (Figure 3b) confirms the cleavage of the C-tail into smaller fragments (Renthal et al., 1983; Ovchinnikov et al., 1984). The large number of peaks obtained by analysis of the supernatant after 24-h digestion (Figure 3d) is due to the greater amount of material cleaved and to self-digestion of papain (the latter was confirmed by incubation of papain in the digestion medium without bacteriorhodopsin).

FTIR Analysis of Bacteriorhodopsin after Papain Digestion. Changes in the FTIR spectra of purple membranes may be correlated with the removal of the C-tail after 2-h papain digestion and, after 24 h, the removal of the N-terminus and a loop (amino acids 66–72) between transmembrane segments 2 and 3. Our visible absorption and fluorescence emission data suggest that the digestion protocol did not cause major conformational changes in the segments remaining associated with the membrane. Thus, any differences in the FTIR spectra produced after digestion must be caused by the absence of the absorptions of the C-tail, N-terminus, and loop 66–72.

The effects of 2-h digestion using papain were an increase in the amide I band maximum from 1661 to 1663–1664 cm^{-1} (revealed in the derivative and deconvolved spectra) and a narrowing of the amide I band. All available data are consistent with the removal of the C-tail during this period (Ovchinnikov et al., 1984; our data above). The spectroscopic changes may be due to the removal of the absorptions of random-coil segments that overlap with the absorption of the α-helices in the spectrum of the native membrane. A shift in the position of random-coil absorptions may be effected by hydrogen–deuterium exchange, which results in a similar shift to higher frequencies for the main helical absorption. The FTIR data suggest therefore that the C-tail of bacteriorhodopsin has a random-coil conformation in the native membrane. This is in agreement with several other studies of the structure of bacteriorhodopsin after proteolytic cleavage including electron and X-ray diffraction (Wallace & Henderson, 1982) and CD (Jap et al., 1983; Wallace & Kohl, 1984). The bands near 1636 and 1680–1690 cm^{-1}, which we assign to β-structure, remain after 2-h digestion (Figures 4b,c and 5). The reduction in intensity of the 1641-cm^{-1} component in the deconvolved spectrum may be due to narrowing of the main amide I band caused by removal of random-coil absorptions and a consequent reduction in band overlap.

Upon further treatment with papain (up to 24 h) the decrease in relative intensity of the 1641- and 1682-cm^{-1} bands in the deconvoluted spectrum may occur as a result of reduced band overlap as above or be indicative of the removal of antiparallel β-structure (Susi et al., 1967; Susi, 1969). However, no reduction in the relative intensity of these absorptions was seen in the second-derivative spectra (Figures 4b and 5), which suggests that bacteriorhodopsin still contains antiparallel β-strand after 24-h digestion. The interpretation of changes in

the relative intensity of minor band components that are revealed by derivative and deconvolution methods is difficult and artifacts may be introduced by changes in bandwidth. It remains safe to conclude that at least some of the antiparallel β-strand detected by FTIR spectroscopy of bacteriorhodopsin is not associated with the C-tail, the N-terminus, or the loop between transmembrane segments 2 and 3.

The absence of any major changes in the FTIR spectrum even after 24-h digestion with papain suggests that the conformation of the remaining portions of bacteriorhodopsin is unaffected by the removal of the cleaved segments. Electron and X-ray diffraction studies have shown that removal of the C-tail by trypsin results in no change in the protein (Wallace & Henderson, 1982). The observed shift in the fluorescence emission maximum is probably due to the exposure of tryptophan residues to the aqueous medium after digestion. According to published models of the arrangement of amino acids across the membrane (Ovchinnikov et al., 1979; Engelman et al., 1980) a majority of the tryptophan residues are located near the membrane surface. Changes in the visible absorption are probably due to changes in polarity in the region of the retinal binding site. The absence of major conformational changes suggested by the FTIR spectra after papain digestion is in agreement with data showing that bacteriorhodopsin continues to pump protons after removal of the C-tail (Abdulaev et al., 1978; Liao & Khorana, 1984; Ovchinnikov et al., 1986).

ACKNOWLEDGMENTS

We thank Christine Hall for expert technical assistance and Michael Cairns for assistance with the HPLC measurements.

Registry No. D_2, 7782-39-0.

REFERENCES

Abdulaev, N. G., Feigina, M. Yu., Kiselev, A. V., Ovchinnikov, Yu. A., Drachev, L. A., Kaulen, A. D., Khitrina, L. V., & Skulachev, V. P. (1978) *FEBS Lett. 90*, 190–194.

Alix, A. J. P., Bernard, L., & Manfait, M., Eds. (1985) *Spectroscopy of Biological Molecules*, Wiley, Chichester.

Asher, S. M., & Levin, I. W. (1977) *Biochim. Biophys. Acta 468*, 63–72.

Bandekar, J., & Krimm, S. (1979) *Proc. Natl. Acad. Sci. U.S.A. 76*, 774–777.

Bandekar, J., & Krimm, S. (1980) *Biopolymers 19*, 31–36.

Birktoft, J. J., & Blow, D. M. (1972) *Biopolymers 11*, 1001–1020.

Blake, C. C. F., Mair, G. A., North, A. C. T., Phillips, D. C., & Sarma, V. R. (1967) *Proc. R. Soc. London, Ser. B 167*, 365–377.

Blaurock, A. E. (1975) *J. Mol. Biol. 93*, 139–158.

Bridgen, J., & Walker, I. D. (1976) *Biochemistry 15*, 792–798.

Byler, D. M., & Susi, H. (1986) *Biopolymers 25*, 469–487.

Chapman, D., Gomez-Fernandez, J. C., Goni, F. M., & Barnard, M. (1980) *J. Biochem. Biophys. Methods 2*, 315–323.

Chirgadze, Yu. N., & Nevskaya, N. A. (1976) *Biopolymers 15*, 627–636.

Chirgadze, Yu. N., Fedorov, O. V., & Trushina, N. P. (1975) *Biopolymers 14*, 679–694.

Cortijo, M., Alonso, A., Gomez-Fernandez, J. C., & Chapman, D. (1982) *J. Mol. Biol. 157*, 597–618.

Cowgill, J. W. (1963) *Biochim. Biophys. Acta 75*, 272–273.

Downer, N. W., Bruchman, T. J., & Hazzard, J. H. (1986) *J. Biol. Chem. 261*, 3640–3647.

Dwivedi, A. M., & Krimm, S. (1984) *Biopolymers 23*, 923–943.

Engelman, D. M., Henderson, R., McLachlan, A. D., & Wallace, B. A. (1980) *Proc. Natl. Acad. Sci. U.S.A. 77*, 2023–2027.

Englander, J. J., Downer, N. W., & Englander, S. W. (1982) *J. Biol. Chem. 257*, 7982–7986.

Gerber, G. E., Gray, Ch. P., Wildenauer, D., & Khorana, H. G. (1977) *Proc. Natl. Acad. Sci. U.S.A. 74*, 5426–5430.

Gerber, G. E., Anderegg, R. Y., Herlihy, W. C., Gray, Ch. P., Biemann, K., & Khorana, H. G. (1979) *Proc. Natl. Acad. Sci. U.S.A. 76*, 227–231.

Govindjee, R., Ohno, K., & Ebrey, T. G. (1982) *Biophys. J. 38*, 85–87.

Haris, P. I., Lee, D. C., & Chapman, D. (1986) *Biochim. Biophys. Acta 874*, 255–265.

Henderson, R. (1975) *J. Mol. Biol. 93*, 123–138.

Henderson, R., & Unwin, P. N. T. (1975) *Nature (London) 257*, 28–32.

Honig, B., Greenberg, A. D., Din, U., & Ebrey, J. G. (1976) *Biochemistry 15*, 4593–4599.

Huang, K.-S., Bayley, H., Liao, M.-J., London, E., & Khorana, H. G. (1981) *J. Biol. Chem. 256*, 3802–3809.

Irving, C., Byers, F., & Leermakers, P. A. (1970) *Biochemistry 9*, 858–864.

Jap, B. K., Maestre, M. F., Hayward, S. B., & Glaeser, R. M. (1983) *Biophys. J. 43*, 81–89.

Katre, N. V., & Stroud, R. M. (1981) *FEBS Lett. 136*, 170–174.

Katre, N. V., Wolber, P. K., Stoeckenius, W., & Stroud, R. M. (1981) *Proc. Natl. Acad. Sci. U.S.A. 78*, 4068–4072.

Kauppinen, J. K., Moffat, D. J., Mantsch, H. H., & Cameron, D. G. (1981) *Appl. Spectrosc. 35*, 271–276.

Khorana, H. G., Gerber, G. E., Herlihy, W. C., Gray, Ch. P., Anderegg, R. J., Nehei, K., & Bieman, K. (1979) *Proc. Natl. Acad. Sci. U.S.A. 76*, 5046–5050.

Kimura, K., Mason, T. L., & Khorana, H. G. (1982) *J. Biol. Chem. 257*, 2859–2867.

Koenig, J. L., & Tabb, D. L. (1980) in *Analytical Applications of FTIR to Molecular and Biological Systems* (Durig, J. R., Ed.) pp 241–255, Reidel, Holland.

Konev, S. V. (1967) *Fluorescence and Phosphorescence of Proteins and Nucleic Acids*, Plenum, New York.

Krimm, S. (1962) *J. Mol. Biol. 4*, 528–540.

Krimm, S., & Abe, Y. (1972) *Proc. Natl. Acad. Sci. U.S.A. 69*, 2788–2792.

Krimm, S., & Dwivedi, A. M. (1982) *Science (Washington, D.C.) 216*, 407–408.

Laemmli, U. K. (1970) *Nature (London) 227*, 680–685.

Lee, D. C., & Chapman, D. (1986) *Bioscience Rep. 6*, 235–256.

Lee, D. C., Hayward, J. A., Restall, C. J., & Chapman, D. (1985) *Biochemistry 24*, 4364–4373.

Lewis, B. A., Harbison, G. S., Herzfeld, J., & Griffin, R. G. (1985) *Biochemistry 24*, 4671–4679.

Liao, M.-J., & Khorana, H. G. (1984) *J. Biol. Chem. 259*, 4194–4199.

Long, M. M., Urry, D. W., & Stoeckenius, W. (1977) *Biochem. Biophys. Res. Commun. 75*, 728–731.

Lozier, R. H., Bogomolni, R. A., & Stoeckenius, W. (1975) *Biophys. J. 15*, 955–962.

Mowerey, P. C., Lozier, R. H., Chae, Q., Iseng, Y.-W., Taylor, M., & Stoeckenius, W. (1979) *Biochemistry 18*, 4100–4107.

Muccio, D. D., & Cassim, J. Y. (1979) *Biophys. J. 26*, 427–440.

Nabedryk, E., Bardin, A. M., & Breton, J. (1985) *Biophys. J. 48*, 873–876.
Nakanishi, K., Balogh-Nair, V., Arnaboldi, M., Tsujimoto, K., & Honig, B. (1980) *J. Am. Chem. Soc. 102*, 7945–7947.
Oesterhelt, D., & Stoeckenius, W. (1971) *Nature (London), New Biol. 233*, 149–152.
Oesterhelt, D., & Stoeckenius, W. (1974) *Methods Enzymol. 31*, 667–678.
Oesterhelt, D., & Hartman, R. (1979) in *Membrane Biochemistry* (Carafoli, E., & Semenza, G., Eds.) pp 154–163, Springer, Berlin.
Olinger, J. M., Hill, D. M., Jakobsen, R. J., & Brody, R. S. (1986) *Biochim. Biophys. Acta 869*, 89–98.
Ovchinnikov, Yu. A., Abdulaev, N. G., Feigina, M. Yu., Kiselev, A. V., & Lobanov, N. A. (1979) *FEBS Lett. 100*, 219–224.
Ovchinnikov, Yu. A., Abdulaev, N. G., & Kiselev, A. V. (1984) in *Biological Membranes* (Chapman, D., Ed.) Vol. 5, pp 193–214, Academic, London.
Ovchinnikov, Yu. A., Abdulaev, N. G., Kiselev, A. V., Drachev, L. A., Kaulen, A. D., & Skulachev, V. P. (1986) *FEBS Lett. 194*, 16–20.
Purcell, J. M., & Susi, H. (1984) *J. Biochem. Biophys. Methods 9*, 193–199.
Renthal, R., Dawson, N., Tuley, J., & Horowitz, P. (1983) *Biochemistry 22*, 5–12.
Rothschild, K. J., & Clark, N. A. (1979) *Science (Washington, D.C.) 204*, 311–312.
Ruegg, M., Metzger, V., & Susi, H. (1975) *Biopolymers 14*, 1465–1471.
Stoeckenius, W., Lozier, R. H., Bogomolni, R. A. (1979) *Biochim. Biophys. Acta 505*, 215–278.
Susi, H. (1969) in *Structure and Stability of Biological Macromolecules* (Timasheff, S. N., & Fasman, G. D., Eds.) pp 573–633, Marcel Dekker, New York.
Susi, H. (1972) *Methods Enzymol. 26*, 455–472.
Susi, H., & Byler, D. M. (1983) *Biochem. Biophys. Res. Commun. 115*, 391–397.
Susi, H., Timasheff, S. N., & Stevens, L. (1967) *J. Biol. Chem. 242*, 5460–5466.
Suzuki, H., Komatsu, T., & Katajima, H. (1974) *J. Phys. Jpn. 37*, 177–185.
Timasheff, S. N., Susi, H., & Stevens, L. (1967) *J. Biol. Chem. 242*, 5467–5473.
Tokunaga, F., & Iwasa, T. (1982) *Methods Enzymol. 88*, 163–167.
Unwin, P. N. T., & Henderson, R. (1975) *J. Mol. Biol. 94*, 425–440.
Walker, J. E., Carne, A. F., & Schmitt, H. W. (1979) *Nature (London) 278*, 653–654.
Wallace, B. A., & Henderson, R. (1982) *Biophys. J. 39*, 233–239.
Wallace, B. A., & Kohl, N. (1984) *Biochim. Biophys. Acta 777*, 93–98.
Yang, W.-J., Griffiths, P. R., Byler, D. M., & Susi, H. (1985) *Appl. Spectrosc. 39*, 282–287.

Monoclonal Antibodies That Bind the Renal Na^+/Glucose Symport System. 1. Identification†

Jin-Shyun Ruth Wu and Julia E. Lever*
Department of Biochemistry and Molecular Biology, The University of Texas Medical School, Houston, Texas 77225
Received October 13, 1986; Revised Manuscript Received May 12, 1987

ABSTRACT: Phlorizin is a specific, high-affinity ligand that binds the active site of the Na^+/glucose symporter by a Na^+-dependent mechanism but is not itself transported across the membrane. We have isolated a panel of monoclonal antibodies that influence high-affinity, Na^+-dependent phlorizin binding to pig renal brush border membranes. Antibodies were derived after immunization of mice either with highly purified renal brush border membranes or with apical membranes purified from LLC-PK_1, a cell line of pig renal proximal tubule origin. Antibody 11A3D6, an IgG_{2b}, reproducibly stimulated Na^+-dependent phlorizin binding whereas antibody 18H10B12, an IgM, strongly inhibited specific binding. These effects were maximal after 30-min incubation and exhibited saturation at increased antibody concentrations. Antibodies did not affect Na^+-dependent sugar uptake in vesicles but significantly prevented transport inhibition by bound phlorizin. Antibodies recognized a 75-kDa antigen identified by Western blot analysis of brush border membranes, and a 75-kDa membrane protein could be immunoprecipitated by 18H10B12. These properties, taken together with results in the following paper [Wu, J.-S. R., & Lever, J. E. (1987) *Biochemistry* (following paper in this issue)], provide compelling evidence that the 75-kDa antigen recognized by these antibodies is a component of the renal Na^+/glucose symporter.

Transporters localized in apical membranes of renal proximal tubule and intestinal epithelial cells catalyze the coupled translocation of glucose and Na^+ in a symport (cotransport) mechanism (Crane, 1977). Renal and intestinal glucose symporters share many functional similarities including substrate specificity and inhibition by the nontranslocated, fully competitive ligand phlorizin. However, certain differences in functional properties have been noted, and there is no evidence that they are identical molecular species [reviewed in Semenza et al. (1984)]. Furthermore, renal and intestinal epithelia may each contain more than one type of Na^+/glucose symporter differing in Na^+/glucose stoichiometries and affinity for phlorizin (Turner & Moran, 1982; Kaunitz et al., 1982).

†This work was supported by U.S. Public Health Service Grant AM27400. J.E.L. is the recipient of NIH Research Career Development Award KO4 AM00768.
* Correspondence should be addressed to this author.

0006-2960/87/0426-5783$01.50/0